Reorientational Dynamics of Amide Ions in Isotypic Phases of Strontium and Calcium Amide. 1. Neutron Diffraction Experiments

J. Senker[†] **and H. Jacobs***

Lehrstuhl für Anorganische Chemie I der Universität Dortmund, D-44221 Dortmund, Germany

M. Müller[‡] **and W. Press**

Institut für Experimentalphysik der Universität Kiel, D-24098 Kiel, Germany

P. Müller

Institut für Anorganische Chemie der RWTH Aachen, D-52056 Aachen, Germany

H. M. Mayer

Institut für Kristallographie der Universität Tübingen, D-72070 Tübingen, Germany, c/o Hahn-Meitner Institut Berlin, Glienicker Strasse 100, D-14109 Berlin, Germany

R. M. Ibberson

ISIS, Rutherford Appleton Laboratory, Chilton OX11 0QX, United Kingdom

Received: September 5, 1997; In Final Form: November 11, 1997

Strontium and calcium amide are ionic compounds crystallizing in a tetragonally distorted anatase structure type. They include asymmetrically charged amide ions (NH_2^-/ND_2^-) which resemble water molecules in their structure and in their charge distribution. By means of temperature-dependent X-ray scattering measurements an anomalous thermal expansion was observed for both compounds (295 K for $Sr(ND_2)_2$, 370 K for $Ca(ND_2)_2$). Fourier analyses based on high-resolution neutron powder diffraction experiments carried out in a large temperature range show especially for the deuterium atoms a remarkably large, anisotropic spatial distribution of the probability density function. It is caused by strongly anisotropic librations of the amide ions. The amplitudes of their normal librations were analyzed using a rigid-body model to parametrize the atomic mean-square displacements of the atoms belonging to the amide ions. They can be described as composed of strong rocking librations with weak temperature dependence and a weak wagging libration with strong temperature dependence.

Introduction

Ionic compounds of alkali and alkaline earth metals containing asymmetrically charged anions often show a large variety of different crystalline phases as a function of temperature. Many of these compounds exist in high-temperature modifications of high symmetry though the molecular anions usually have low symmetry. This can be achieved only as an ensemble average caused by orientational disorder of the molecular anions.

Detailed studies of phase transitions between low- and high-temperature phases as well as of rotational and translational dynamics of molecular anions were mainly performed for small linear and tetrahedral molecular groups. Well-known examples are alkali metal hydroxides,[1−11] hydrogensulfides,[12−18] and ammonium halides.[19−23] The type of motion and the resulting probability density function[54] strongly depend on the crystalline structure and on the symmetry and magnitude of the potential at the site of the molecular groups.

Amide ions (NH_2^-) are isoelectronic with water molecules (OH_2). Therefore, alkali and alkaline earth metal amides are of great interest as simple model compounds for the understanding of molecular dynamics in water-containing systems. So far, these compounds—especially the alkaline earth metal amides—have not been studied in a systematic manner. Probably, this is due to their high air sensitivity, which must be mastered in preparation and handling. We have chosen four alkali and alkaline earth metal amides to perform an extended study of dynamical processes of amide ions in these compounds in a collaborative effort of two groups in Kiel and Dortmund.[24−26] In this cooperation we combine different analytical methods such as quasielastic neutron scattering (QNS) and inelastic neutron scattering (INS) as well as solid-state NMR spectroscopy in order to investigate molecular dynamics in a very large range of time scales (10^{-3}−10^{14} Hz).

However, the study of dynamical processes in solid materials must be based on a detailed knowledge of the static structure, the probability density function, and its temperature dependence. An accurate determination of all atomic positions including those of the hydrogen atoms is the main purpose of the present work on strontium and calcium amide. Earlier structure determina-

[†] Present address: Experimentalphysik II der Universität Bayreuth, D-95440 Bayreuth, Germany.

[‡] Current address: Institut Laue-Langevin, B. P. 156, F-38036 Grenoble Cedex 9, France.

S1089-5647(97)02907-6 CCC: $15.00
Published on Web 01/22/1998

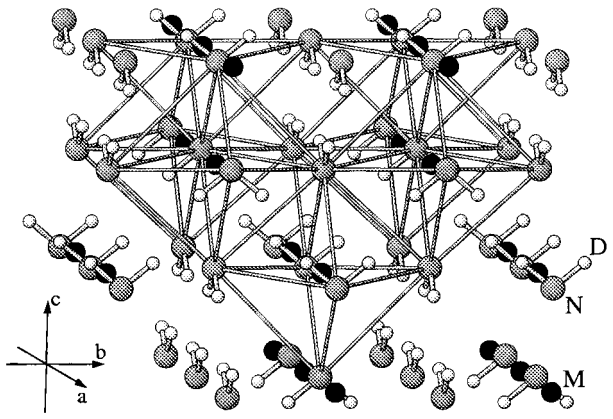

Figure 1. Part of the structure of $Sr(ND_2)_2$ and $Ca(ND_2)_2$ including the amide ion orientation. It can be described by a distorted cubic close packing of amide ions with cations occupying half of the octahedral sites. Each cation has four cation neighbors forming a tetrahedron. The hydrogen atoms are distributed in "empty" octahedra of the amide ion packing. Further crystallographic informations are listed below (cited from ref 27). The space group type is $I4_1/amd$ (No. 141). The site of the cations is 4a (0 $^3/_4$ $^1/_8$), the site of the nitrogen atoms is 8e (0 $^1/_4$ 0.115) and the site of the deuterium atoms is 16h (0.158 1/4 0.160).

tions lead to an anatase structure type with a tetragonal cell for both compounds[27−30] (see Figure 1). Considering the nearly ideal ratio of the crystal axes ($c/a = 2.00$) only small, twinned crystals can be grown[30] which are not suitable for single crystal neutron diffraction investigations. The present experiments, therefore, were based on powder diffraction. We carried out high-resolution neutron powder and Guinier X-ray diffraction experiments in a large temperature range using fully deuterated compounds ($Sr(ND_2)_2$/$Ca(ND_2)_2$). The observed structure factors were extracted from the neutron diffraction pattern and Fourier analyses were made with these data to characterize the probability density function especially of the amide ions in detail.

Dynamical investigations by means of QNS and ^{2}H NMR measurements will be presented in a forthcoming paper.

Experimental Details

Preparation and Characterization. Protonated and deuterated samples of calcium and strontium amide were prepared by reaction of calcium (Alfa Products Johnson Mathey GmbH, Frankfurt, 99.5%), strontium (Alfa Products Johnson Mathey GmbH, Frankfurt, 99%) metal and liquid ammonia (Messer Griesheim, Frankfurt, 99.999%), deuteroammonia (MSD Isotopes, Merc Frost, Canada, 99.4%):

$$M + 2NX_3 \rightarrow M(NX_2)_2 + X_2 \; (M = Ca, Sr; X = H, D)$$

In this reaction NH_3/ND_3 was used as reactant and solvent for metals and amides. We recognized that the use of large amounts of metal does not lead to a quantitative conversion. Samples of high purity and good crystallinity were achieved by use of small amounts of calcium and strontium (≈20 mmol) and a large excess of NH_3/ND_3 (≈400 mmol). The reaction components were heated to 370 K for 2 weeks. The metals as well as the corresponding amides are highly sensitive against moisture, carbon dioxide, and oxygen. Therefore, all handling of the starting materials and the products must be performed under inert gas (argon, Messer Griesheim, Krefeld, 99.998%) in a self-made glovebox.[31] At the reaction temperature the vapor pressure of the solvent is about 60 bar, and so the reaction was carried out in a stainless steel autoclave (material no. 1.3971).[32]

TABLE 1: Unit-Cell Parameters Based on X-ray Powder Data, Volume of One Formula Unit (V_Z), and Calculated Radiographic as Well as Measured Mass Densities (ρ_X, ρ)

		$Ca(NH_2)_2$	$Ca(ND_2)_2$	$Sr(NH_2)_2$	$Sr(ND_2)_2$
cell parameters (Å)	*a*	5.143(5)	5.141(1)	5.453(4)	5.452(4)
	c	10.300(9)	10.287(2)	10.904(9)	10.876(8)
cell parameters (Å)	*a*	5.147(3)		5.451(5)	5.459(3)
in refs 27, 30	*c*	10.294(7)		10.910(9)	10.886(7)
V_z (Å^3)		68.1(1)	68.0(1)	81.1(1)	80.8(2)
ρ_x (g/cm^3)			1.86(1)		2.54(2)
ρ (g/cm^3)			1.85(1)		2.57(1)

This enables work at pressures up to 100 bar. A valve allows us to fill up the closed autoclave with the reaction gas by cooling it in a mixture of dry ice and acetone. The amount of the reaction gas was determined in a Hüttig−Tensieudiometer.[33] After the reaction was completed remaining solvent was simply evaporated, and the autoclave was opened within the glovebox.

For characterization and in order to check for crystalline impurities Debye−Scherrer powder patterns using the method of Straumanis with Cu Kα radiation were made of all compounds. To protect the samples against decomposition during the measurements we filled thin glass capillaries (i.d. = 0.3 mm), and after locking them out of the glovebox they were immediately sealed off. The powder patterns could be completely indexed within the above-mentioned tetragonal metric. The cell parameters were determined by a calculation using a compensation algorithm[34] and are reported in Table 1, along with the mass densities of the deuterated compounds, which were measured by means of a gas pycnometer (AccuPyc 1330, Micrometrics, Neuss; see Table 1). They are in good agreement with the radiographic densities calculated from the cell parameters listed in Table 1. Furthermore, the reflection intensities estimated of the Debye−Scherrer powder patterns fit well to the calculated intensities from the results listed ref 27.

Main products of the decomposition of calcium and strontium amide and of the educts getting in contact with air are carbonates, hydrogencarbonates, and hydroxides as well as their hydrates. These compounds contain molecular groups showing characteristic vibration bands in IR absorption and Raman scattering spectra already referenced in the literature.[35] For these reasons we did IR and Raman spectroscopic investigations to check the compounds for such impurities as well. The samples for the IR absorption measurements using an IFS 113v Fourier spectrometer (Bruker, Karlsruhe) were pulverized in a large excess of dried KBr and then pressed. To protect them against decomposition, they must be completely enclosed in dried KBr. We used a sandwich technique for the compacts: the outer layers contain pure KBr and the inner layer contains the KBr/sample trituration. For the Raman scattering experiments a SAT64000 spectrometer equipped with an argon laser (Spectraphysics) was used. Again the compounds were filled into glass capillaries (i.d. = 1.0 mm) which were sealed off. Observed vibration bands and their assignments are listed in Table 2.

Possible splittings of the internal modes of amide ions in calcium and strontium amide under the influence of crystal symmetry were analyzed by means of a factor group analysis using the correlation method.[38] This analysis is based on crystallographic data resulting from our neutron diffraction experiments (see Table 5 and 6) and is shown in Figure 2. By these results we were able to assign all vibration bands definitely and to explain a weak additional band in the Raman spectra of $Ca(NH_2)_2$ as Davidov splitting of the symmetric stretching vibration. The IR and Raman spectra of the deuterated compounds show as well very weak bands of stretching

TABLE 2: Observed Vibration Bands in the Frequency Range of the Stretching and Deformation Vibrations of Calcium and Strontium Amide (vw = Very Weak; w = Weak; m = Medium; st = Strong; vst = Very Strong; unc = Uncoupled Vibration of the NHD^- Ions)

	ν/cm^{-1}			ref 36 and
	IR	Raman	assignment	37 ν/cm^{-1}
$Ca(NH_2)_2$	3294 (st)	3307 (m)	$\nu_{as}(NH_2)$	3295 (m)
		3258 (w)	$\nu_s(NH_2)$	
	3231 (st)	3235 (st)	$\nu_s(NH_2)$	3233 (st)
	1517 (vst)	1535 (w)	$\delta(NH_2)$	1517 (st)
$Sr(NH_2)_2$	3267 (st)	3270 (m)	$\nu_{as}(NH_2)$	3269 (st)
	3205 (st)	3206 (st)	$\nu_s(NH_2)$	3207 (vst)
	1509 (vst)	1526 (w)	$\delta(NH_2)$	1511 (st)
$Ca(ND_2)_2$	3264 (vw)	3271 (vw)	$\nu_{unc}(NH)$	
	2450 (w)	2458 (st)	$\nu_{as}(ND_2)$	2449 (m)
	2371 (st)	2373 (vst)	$\nu_s(ND_2)$	2366 (st)
		1124 (vw)	$\delta(ND_2)$	
	1117 (vst)	1097 (w)	$\delta(ND_2)$	1155 (st)
$Sr(ND_2)_2$	3237 (w)	3237 (vw)	$\nu_{unc}(ND)$	
	2433 (st)	2436 (m)	$\nu_{as}(ND_2)$	
	2391 (w)	2387 (vw)	$\nu_{unc}(ND)$	
	2353 (vst)	2355 (vst)	$\nu_s(ND_2)$	
	1113 (vst)	1101 (w)	$\delta(ND_2)$	

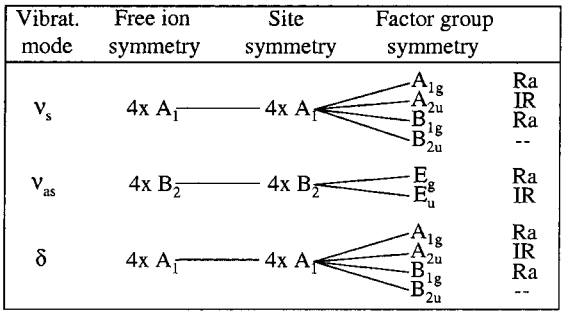

Figure 2. Correlation table for the stretching and deformation vibrations of the amide ions in calcium and strontium amide (IR/Ra: expected to be observed in the infrared/Raman spectra).

vibrations of NHD^- ions (see Table 2). A comparison of these band intensities with those of ND_2^- ions shows that a percentage of hydrogen atoms below 2% were received in the deuterated compounds.

Furthermore, we carried out specific heat measurements with the deuterated compounds in a temperature range between 100 and 500 K using a DSC-Pyris 1 (Perkin-Elmer).

X-ray and Neutron-Scattering Investigations. Most of our neutron powder diffraction experiments were carried out at the Hahn-Meitner Institute using the Flate-cone and conventional powder diffractometer E2.[39] The samples were mounted in a standard cryofurnace (orange type). We chose an incident wavelength of $\lambda = 1.21$ Å and used collimators with a divergence of 10′ and 30′ which were placed between the monochromator and reactor. The data were collected by a multicounter with an angular range of 80° in the scattering angle and a distance between the individual detector channels of 0.2°. Two runs were made for each diffractogram varying the starting angle by 0.1° to get a satisfactory number of points on a single reflection in the powder pattern. Although parasitic scattering from the aluminum walls of the furnace was reduced by an oscillating radial collimator, the two most intense aluminum reflections (1 1 1) and (2 0 0) were observed. Because of the fact that this scattering does not occur in the center of the cryostat, these reflections could not be handled with a simultaneous Rietveld refinement of a second phase. Either they were fitted separately and subtracted from the diffractogram or the whole region including reflections of the samples were excluded from the refinement.

Additionally, we obtained high-resolution neutron diffractograms of $Sr(ND_2)_2$ for three temperatures with the time-of-flight (TOF) diffractometer HRPD[40] at the ISIS facility ($\Delta d/d = 4 \times 10^{-4}$ in backscattering geometry). The great advantage of a TOF diffractometer at a spallation source in contrast to a conventional diffractometer like the E2 is the constant resolution $\Delta d/d$, where d is the lattice spacing. So higher order reflections which are broadened at a conventional diffractometer remain sharp in this case and could easily be resolved and separated from the background. The range of scattering vectors could be extended to larger values, and so the accuracy of our analyses (especially for Fourier maps) was increased. Again the samples were mounted in a cryofurnace, but in contrast to the cryostat used at E2 it was equipped with vanadium windows to avoid unwanted reflections.

For all neutron diffraction experiments the pulverized samples were filled into cylindrical vanadium cans (i.d. = 8 mm) which were sealed by gold rings.

In addition to the neutron diffraction experiments Guinier diffraction measurements were carried out on $Sr(ND_2)_2$. For temperatures below room temperature a Huber G642 (Rimsting, Germany) instrument and above room temperature a Huber G644 diffractometer were used. The first instrument works with flat-plate samples mounted in a ^{4}He-closed-cycle cryostat. We used Kapton foil 200HN (thickness = 50 μm, August Krempel Soehne GmbH & Co, Enzweihingen, Germany) as a transmission window to protect the samples against decomposition. For the second instrument the sample environment is the same as for the Debye−Scherrer measurements. Both diffractometers work in transmission geometry with Cu Kα_1 ($\lambda = 1.540\,56$ Å) radiation.

To obtain the temperature dependence of the lattice parameters for calcium amide a Simon-Guinier camera (Cu Kα_1 radiation) was used. As for the Debye−Scherrer powder patterns, the X-ray photographs were indexed and the cell parameters were calculated.[34]

All powder diffraction data were analyzed using the least-squares program GSAS[41] which is based on Rietveld methods.[42−44] It is suitable for the refinement of data collected at conventional as well as TOF diffractometers and for the simultaneous refinement of several data sets belonging to different types of radiation and diffraction geometries. GSAS provides a set of profile functions for each type of data set and allows the standard structure refinement including anisotropic mean-square (m.-s.) displacement parameters for each atom and further the parametrization of structural parameters in a rigid-body. We fitted the E2 data using a standard Gaussian profile modified for peak asymmetry.[44] For the Guinier diffractograms a multiterm Simpson's rule integration of a pseudo-Voigt function[45] was used and for the time-of-flight data from HRPD the profile was described by a convolution of two back-to-back exponentials with a pseudo-Voigt function.[41] Instrument dependent profile parameters were determined by calibration measurements using Si ($a = 5.4306$ Å) and CaF_2 ($a = 5.4631$ Å) samples. Furthermore, we treated the background with a cosine Fourier series including a constant leading term and corrected short period fluctuations associated with static or dynamical disorder or due to stray scattering into neighboring channels in a multicounter with background points manually set. For temperatures where both X-ray and neutron diffraction data were available they were refined simultaneously.

TABLE 3: Unit-Cell Parameters and Volume of $Sr(ND_2)_2$ Determined in Complete Rietveld Profile Analyses of Guinier Diffraction Measurements Using Cu $K\alpha_1$ Radiation

T/K	*a*/Å	*c*/Å	*V*/Å^3
70	5.441(1)	10.877(2)	322.0(1)
140	5.445(1)	10.878(2)	322.5(1)
190	5.447(1)	10.875(2)	322.7(1)
250	5.451(1)	10.876(2)	323.2(1)
294	5.454(1)	10.873(2)	323.4(1)
320	5.457(1)	10.879(2)	324.0(1)
360	5.462(1)	10.885(2)	324.8(1)
460	5.474(1)	10.904(2)	326.7(1)

TABLE 4: Unit-Cell Parameters and Volume of $Ca(ND_2)_2$ Determined Using a Simon-Guinier Camera with Cu $K\alpha_1$ Radiation

T/K	*a*/Å	*c*/Å	*V*/Å^3
303	5.139(1)	10.298(3)	272.0(1)
323	5.140(1)	10.300(3)	272.1(1)
343	5.141(1)	10.301(3)	272.3(1)
363	5.142(1)	10.305(3)	272.5(1)
383	5.146(1)	10.298(3)	272.7(1)
403	5.149(1)	10.304(3)	273.2(1)
363	5.151(1)	10.309(3)	273.5(1)
443	5.155(1)	10.316(3)	274.1(1)
463	5.158(1)	10.318(3)	274.5(1)

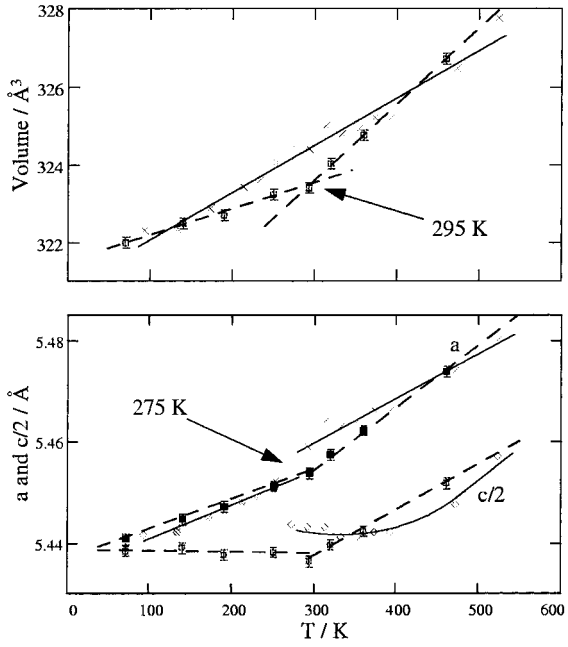

Figure 3. Thermal expansion of the cell parameters and volume of $Sr(ND_2)_2$. Simon-Guinier data of Nagib, Kistrup, and Jacobs:[27] The *a*-axis as well as the cell volume are marked as [×] and half of the *c*-axis is marked as [◇]. The solid, black lines show the trends of these data. Guinier diffraction data: The *a*-axis is marked as [■], and half of the *c*-axis as well as the cell volume are marked as [□]. The solid, dashed lines represent the trends of these data.

Results and Discussion

Lattice parameters and cell volumes of $Sr(ND_2)_2$ and $Ca(ND_2)_2$ were determined for various temperatures. The methods used for it are described in the previous section. Our results are listed in Tables 3 and 4, and additionally they are depicted in Figures 3 and 4. We compared cell parameters extracted from Guinier diffractograms by Rietveld analyses (see the previous section) with earlier determined data using a Simon-Guinier camera.[27] Their temperature dependence is similar for both methods, but nevertheless, we obtained some differences probably caused by a systematic error in the evaluation of the Simon-Guinier data.

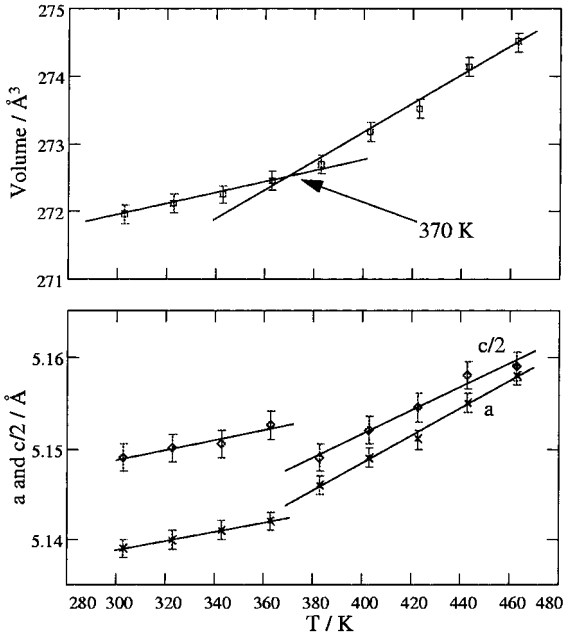

Figure 4. Thermal expansion of the cell parameters and volume of $Ca(ND_2)_2$. The *a*-axis is marked as [×], half of the *c*-axis is marked as [◇], and the cell volume is marked as [□]. The solid, black lines show the trends.

The two most striking points are the temperature independent *c*/*a* ratio of 2.00 for lower temperatures and the strong discontinuity of the lattice parameters near room temperature (abrupt increase of the *a*-axis and simultaneous decrease of the *c*-axis) which were observed only for the lattice parameters extracted from Simon-Guinier measurements. But in fact, even values determined with X-ray diffraction methods show a discrete change of the thermal expansion coefficients (see Figure 3).

These effects can be explained considering the very small difference of *a* and *c*/2 obtained in our diffraction investigations. This leads to a systematic overlap of reflections in a powder pattern if $h^2 + k^2 + l^2/4$ is equal. Only one 2θ value can be extracted from the Simon-Guinier data for those reflections, and thus the evaluation may be corrupted. For this reason reflections of this type were not taken into account for the calculation of the lattice parameters of $Ca(ND_2)_2$ from the Simon-Guinier data (see Figure 4).

The temperature dependence of the lattice parameters and cell volumes is similar for both compounds. In a good approximation the expansion coefficients are constant with a discrete change during the transition. The transition temperatures were determined to be 295 K for $Sr(ND_2)_2$ and 370 K for $Ca(ND_2)_2$ by linear regression analyses of the cell volumes in the low- and high-temperature regions. Within the accuracy of our measurements no discontinuous change of the cell volume could be observed. Specific heat measurements show neither a transition enthalpy nor a discrete change in the specific heat in the temperature range between 100 and 500 K. These results indicate a transition of higher order even though a first-order part seems to be concerned because of a discrete changing of the lattice parameters.

To get further information about the process causing this transition, a complete structure determination including the deuterium atoms in a large temperature range is necessary. For this reason we carried out six neutron powder diffraction experiments for each of both compounds in a temperature range between 80 and 560 K. Three measurements on $Sr(ND_2)_2$ (80,

190, and 550 K) were done using the TOF diffractometer HRPD. Data of all other diffractograms were collected at the conventional diffractometer $E2_1$. We started our Rietveld analyses (see previous section) using the structure model developed by Nagib, Kistrup, and Jacobs (see Figure 1). In this model one site parameter (z) for the nitrogen atoms and two site parameters (x and z) for the deuterium atoms had to be varied. Additionally, we introduced an isotropic m.-s. displacement parameter for each atom in our refinement.

However, in this approximation the achieved quality of the refinements was not sufficient. Calculations of the R Bragg factor R_{F^2} yielded values of 20% for both compounds and all temperatures. For specific reflection groups the Rietveld profile fits show systematic differences. We attempted to improve this situation by considering preferred orientation of platey or needle-shaped crystals with their normal axis and their long axis parallel to {100} and {0 0 1} scattering vectors, respectively. However, without success.

We then carried out Fourier analyses using the observed structure factors of our neutron diffraction data. In centrosymmetric space group types such as $I4_1/amd$ all structure factors are real, which means that all phases must be 0 or π. Nitrogen is the strongest scatterer in our neutron diffraction investigations and hence dominates the calculated structure factors. Furthermore, its position is determined by the present and previous X-ray diffraction studies[27] very well. Therefore, most of the phases calculated with the above-mentioned model are proper, which is not necessarily true for the amplitudes. So it is reasonable to use the calculated phases in our Fourier analyses. The amplitudes of the structure factors were derived by integration over the reflection profile considering intensity correction factors depending on the well-known instrument geometry. The intensity of overlapping reflections was divided into the single reflections taking into account the ratio of the calculated intensities of these reflections. A routine to treat diffraction data in this manner is also provided in the GSAS package.[41]

In two-dimensional Fourier cuts the nuclear density was scanned. The strongly anisotropic spatial distribution of the deuterium atoms along the {100} planes was conspicuous. These planes can be identified with the molecular plane of the amide ions. Obviously, the structure model can be improved by introducing anisotropic m.-s. displacement parameters for the deuterium and the nitrogen atoms. After performing only a few additional refinement runs, we reached a sufficient profile fit. The R Bragg factors R_{F^2} now were in the range of 6% for all temperatures, and the above-mentioned systematic differences for some reflection groups vanished. Within the accuracy of our measurements no further differences in the profile fit could be observed (for example, see Figures 5 and 6). Though we had to consider anisotropic m.-s. displacements for the deuterium and the nitrogen atoms to reach sufficient agreement between observed and calculated intensities, the results of our high-resolution neutron powder diffraction experiments corroborate the structure model developed by Nagib, Kistrup and Jacobs (see Figure 1 and ref 27). For relevant crystallographic information see Tables 5 and 6. The coordination of the amide ions is depicted in Figure 7.

Using the improved structure model we scanned the nuclear density by Fourier cuts again. Phases and amplitudes of the observed structure factors were determined as mentioned above. In contrast to the previous situation, the new model is good and the probability that most of the phases and amplitudes are correctly determined is high. So we should be able to study

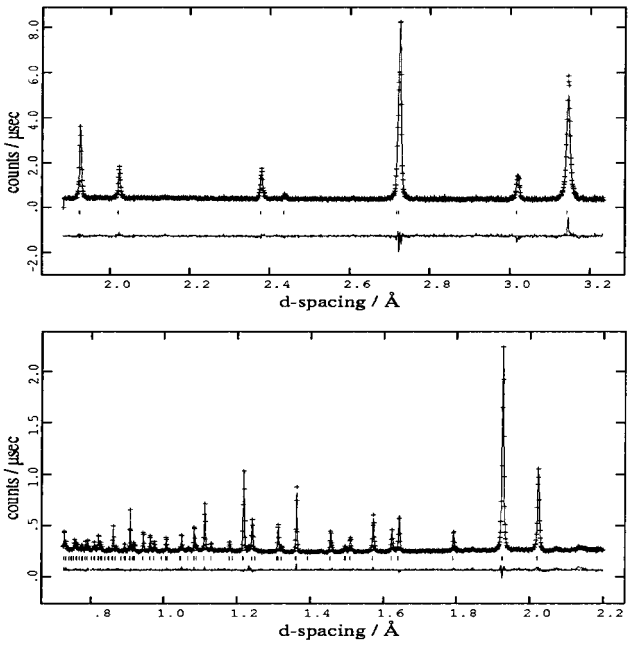

Figure 5. Rietveld profile fits for $Sr(ND_2)_2$ at 190 K. The experiment was carried out at the TOF instrument HRPD of the ISIS facility using a time window of 100 ms for data collection. For larger d spacings we have chosen 80 ms as low limit in a first run. Lower d spacings were measured in a second run with a low limit of 20 ms.

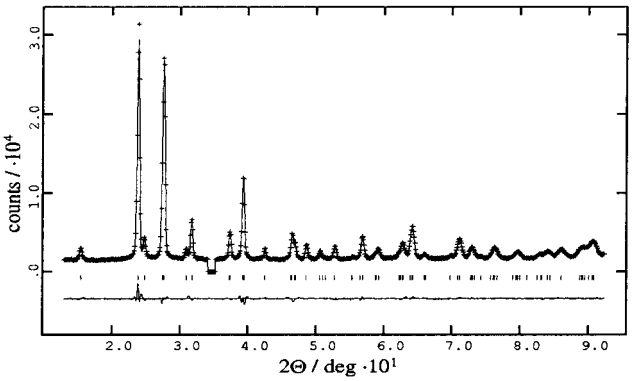

Figure 6. Rietveld profile fit for $Ca(ND_2)_2$ at 200 K. The diffractogram was measured at the instrument $E2_1$ of the HMI Berlin using a wavelength λ of 1.2209 Å and a 10 ft collimator. The region around 35 in 2θ was excluded from the refinement because of aluminum reflections from the cryostat walls.

details of the pdf. In fact the pdf of the amide ions—especially of the deuterons—is smeared out into a large, anisotropic volume element which is aligned along the {100} planes (for example, see Figure 8), indicating that librations of the amide ions are strongly involved in the dynamical processes of these compounds. The amplitude of the rocking libration is clearly larger than the amplitudes of the other normal librations. Even at low temperatures (<100 K) this amplitude is remarkably large. Furthermore, its temperature dependence must be small because of only slight differences of the pdf of the amide ions for low and high temperatures (see Figure 8). The second analysis confirms our previously mentioned results and certifies that the use of anisotropic m.-s. displacement parameters for the nitrogen and deuterium atoms in our refinements are well-suited to approximate the pdf of the amide ions in $Sr(ND_2)_2$ and $Ca(ND_2)_2$.

Due to the large amplitude of the rocking libration, r_{xx} is 3 times larger as the r_{yy} and r_{zz} (see Figure 9 and Tables 5 and 6, respectively). For the deuteron, r_{xx} is positioned in the (010)

TABLE 5: Relevant Crystallographic Refinement Parameters Obtained by Rietveld Profile Fits of the Neutron Diffraction Data of $Sr(ND_2)_2$[a]

	80 K	190 K	293 K	360 K	460 K	550 K
refined site parameter for N on site 8e (0 1/4 *z*)						
z	0.1134(2)	0.1138(6)	0.1141(6)	0.1135(7)	0.1132(7)	0.1133(2)
refined site parameter for D on site 16h (*x* 1/4 *z*)						
x	0.1444(4)	0.1403(5)	0.1393(14)	0.1368(12)	0.1417(16)	0.1371(5)
z	0.1719(2)	0.1710(2)	0.1687(9)	0.1684(6)	0.1675(8)	0.1679(3)
isotropic rms displacement of Sr						
r/Å	0.044(3)	0.114(2)	0.126(10)	0.125(10)	0.164(13)	0.155(3)
anisotropic rms displacement of N						
r_{xx}/Å	0.143(5)	0.199(4)	0.179(7)	0.226(8)	0.246(9)	0.282(6)
r_{yy}/Å	0.015(4)	0.098(4)	0.122(6)	0.154(6)	0.158(7)	0.137(4)
r_{zz}/Å	0.079(6)	0.120(5)	0.153(8)	0.162(9)	0.181(9)	0.147(7)
(α β γ)	(0 0 0)	(0 0 0)	(0 0 0)	(0 0 0)	(0 0 0)	(0 0 0)
anisotropic rms displacement of D						
r_{xx}/Å	0.423(6)	0.464(6)	0.478(12)	0.519(14)	0.544(16)	0.583(7)
r_{yy}/Å	0.132(5)	0.186(5)	0.204(10)	0.226(12)	0.243(12)	0.251(6)
r_{zz}/Å	0.118(5)	0.153(5)	0.161(11)	0.184(13)	0.199(14)	0.209(7)
(α β γ)	(0 325.5 0)	(0 326.1 0)	(0 319.2 0)	(0 321.9 0)	(0 323.2 0)	(0 326.1 0)
bond length and bond angle of an amide ion						
d_{ND}/Å	0.997(3)	0.986(3)	0.966(8)	0.953(8)	0.948(8)	0.943(4)
DND/deg	102.2(4)	101.6(4)	103.8(9)	106.2(9)	105.2(9)	104.1(4)
numerical criteria of fit (R_p, *R* pattern; R_{F^2}, *R* Bragg factor[42])						
R_p/%	3.0	2.6	5.4	5.4	4.7	3.3
R_{F^2}/%	5.7	5.3	5.8	5.9	7.5	6.4

[a] The diffraction patterns collected at the flat-cone diffractometer E2 (HMI Berlin) contain about 80−84 Bragg reflections, while the number of Bragg reflections received at the TOF diffractometer HRPD is in the range of 140. They contribute to the intensity of a number of 50−56 (E2) and 87−90 (HRPD), respectively, the so-called effective reflections. These take the overlapp of some Bragg reflections in the diffraction pattern into account. A procedure of calculating the number of effective reflections is described in ref 42. The thermal displacements of all atoms are listed in terms of the root mean-square (rms) displacements ($r = \sqrt{\langle u^2 \rangle}$). To characterize the anisotropic m.-s. displacement matrices, the average values of *r* along the directions of the three principal axes are given. The orientation of the principal axes system *X*, *Y*, *Z* with respect to the orthonormal crystallographic coordinate system *x*, *y*, *z* is described by the three Eulerian angles α, β, γ. The definition of the Eulerian angles used here is the same as that of Brink and Sachtler,[46] where α, β, γ are introduced as rotation angles through which *X*, *Y*, *Z* have to be rotated, in positive sense first about the *Z*-axis (α), then about the new *Y*′-axis (β) parallel to the *xy*-plane, and final about the new *Z*″-axis (γ).

TABLE 6: Relevant Crystallographic Refinement Parameters Obtained in Rietveld Profile Fits of the Neutron Diffraction Data of $Ca(ND_2)_2$[a]

	100 K	200 K	293 K	380 K	460 K	555 K
refined site parameter for N on site 8e (0 1/4 *z*)						
z	0.1117(2)	0.1120(2)	0.1120(2)	0.1122(3)	0.1119(4)	0.1125(5)
refined site parameter for D on site 16h (*x* 1/4 *z*)						
x	0.1498(7)	0.1498(6)	0.1493(7)	0.1465(11)	0.1438(10)	0.1416(11)
z	0.1709(4)	0.1702(3)	0.1693(4)	0.1682(6)	0.1678(6)	0.1701(7)
isotropic rms displacement of Ca						
r/Å	0.117(4)	0.130(4)	0.128(4)	0.146(5)	0.157(5)	0.180(6)
anisotropic rms displacement of N						
r_{xx}/Å	0.138(6)	0.129(5)	0.148(5)	0.164(7)	0.175(7)	0.211(9)
r_{yy}/Å	0.087(9)	0.114(7)	0.117(8)	0.144(9)	0.170(9)	0.188(11)
r_{zz}/Å	0.110(8)	0.144(7)	0.151(8)	0.157(11)	0.161(11)	0.178(13)
(α β γ)	(0 0 0)	(0 0 0)	(0 0 0)	(0 0 0)	(0 0 0)	(0 0 0)
anisotropic rms displacement of D						
r_{xx}/Å	0.437(12)	0.425(8)	0.443(10)	0.483(12)	0.496(13)	0.531(14)
r_{yy}/Å	0.184(10)	0.204(7)	0.212(8)	0.251(11)	0.275(12)	0.275(13)
r_{zz}/Å	0.128(10)	0.094(7)	0.147(7)	0.164(10)	0.162(10)	0.204(12)
(α β γ)	(0 320.6 0)	(0 319.0 0)	(0 317.5 0)	(0 316.5 0)	(0 316.3 0)	(0 315.9 0)
bond length and bond angle of an amide ion						
d_{ND}/Å	0.985(6)	0.984(6)	0.974(7)	0.952(6)	0.942(7)	0.939(8)
DND/deg	102.8(4)	103.9(4)	104.7(5)	105.1(6)	104.4(6)	101.8(7)
numerical criteria of fit (R_p, *R* pattern; R_{F^2}, *R* Bragg factor[42])						
R_p/%	3.8	2.9	3.0	3.3	3.0	3.0
R_{F^2}/%	5.6	3.4	5.3	5.1	5.2	5.4

[a] The number of effecitve reflections is in the range of 46−50 while the number of Bragg reflections is about 76−79. The same notation as in Table 5 is used.

plane (this plane is also the molecular plane of the corresponding amide ion) and is twisted in positive sense about the angle β to the [100] axis. r_{yy} represents the rms displacement perpendicular to the (010) plane, and r_{zz} is roughly aligned with the ND bond. r_{xx}, r_{yy}, and r_{zz} increase approximately linearly with rising temperature for both compounds (see Figure 9). A similar behavior was observed for the anisotropic rms displacement parameters of nitrogen and the isotropic rms displacement of the metal atoms. The temperature dependence of the rms displacement parameters for all atoms does not show an unusual behavior which can be correlated with a jump of the thermal expansion coefficients (see Figures 3 and 4). Additionally,

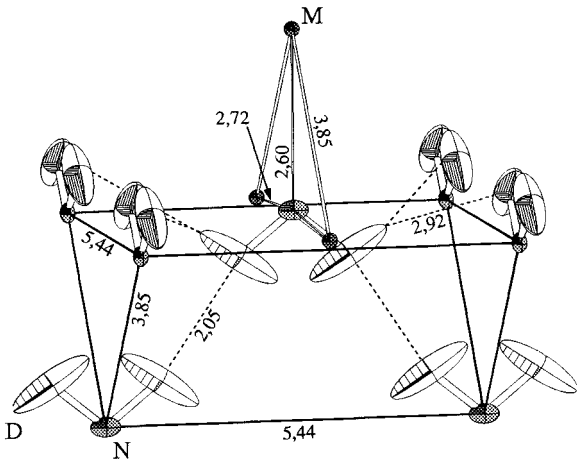

Figure 7. Coordination of amide ions in $Sr(ND_2)_2$ and $Ca(ND_2)_2$. This picture is extracted from the crystallographic data of $Sr(ND_2)_2$ at 80 K (see Table 5). The ellipsoid representation of the anisotropic m.-s. displacement parameters corresponds to 50% probability finding an atom inward the ellipsoid volume.

neither changes of the structure of the amide ions nor of their position in the crystal with temperature are significant for both compounds.

In contrast to this, the results of temperature-dependent deuterium solid-state NMR investigations[26] hint that librational modes of the amide ions are considerably involved in the processes causing the unusual thermal behavior of the cell parameters.

One reason the temperature dependent analysis of the anisotropic thermal displacement parameters does not lead to comparable results may be caused by the assembly of translational, librational and mixed vibrational modes to the m.-s. displacement of each atom in a crystalline compound. Thus, to study the librational modes of the amide ions in more detail, first its contribution to the thermal displacement parameters of the deuterium and nitrogen atoms must be separated. Therefore, we applied a rigid-body model[47,48] to the amide ions. It is sensible only if the amplitudes of the external modes of the amide ions are much larger than their internal vibrations. The knowledge especially of mean amplitudes of internal vibrations of molecules and their corresponding mean-square displacements is of great interest for several modern techniques used for structure determination. A good estimation can be provided by calculating these values from spectroscopic data (Raman and IR).[49] This has already been done for many molecules, and the calculated m.-s. displacements can be looked up in the literature.[49] Typical average amplitudes of internal vibrations for molecules containing ND bonds are in the range of 0.05 Å. They are small enough to justify a rigid-body parametrization of the amide ions in $Sr(ND_2)_2$ and $Ca(ND_2)_2$.

The m.-s. displacements of an amide ion α are described in terms of a translation matrix **T** ($\mathbf{T}(\alpha) = \langle \vec{u}(\alpha)(\vec{u}(\alpha))^T \rangle$) considering only the translational motions of the molecular center, a libration matrix **L** ($\mathbf{L}(\alpha) = \langle \vec{\theta}(\alpha)(\vec{\theta}(\alpha))^T \rangle$), which represents the librational motions, and a correlation matrix **S** ($\mathbf{S}(\alpha) = \langle \vec{u}(\alpha)(\vec{\theta}(\alpha))^T \rangle$) taking into account the existence of mixed modes. The center of mass of the amide ions (we chose it as the molecular center for the parametrization) occupies the site 8e. The symmetry of the point group belonging to this site is C_{2v}. Because of this high symmetry the Cartesian coordinate system used for the description of the translation, libration, and correlation matrices and the principal axes system of inertia of the amide ions are parallel and aligned with the orthonormal crystallographic coordinate system. Therefore, the **T**, **L**, **S** matrices have the form:

$$\mathbf{T}, \mathbf{L} = \begin{pmatrix} xx & 0 & 0 \\ 0 & yy & 0 \\ 0 & 0 & zz \end{pmatrix} \qquad \mathbf{S} = \begin{pmatrix} 0 & xy & 0 \\ yx & 0 & 0 \\ 0 & 0 & 0 \end{pmatrix}$$

In this case, the elements L_{xx}, L_{yy}, and L_{zz} of the libration tensor are equal to the m.-s. amplitudes of the normal librations

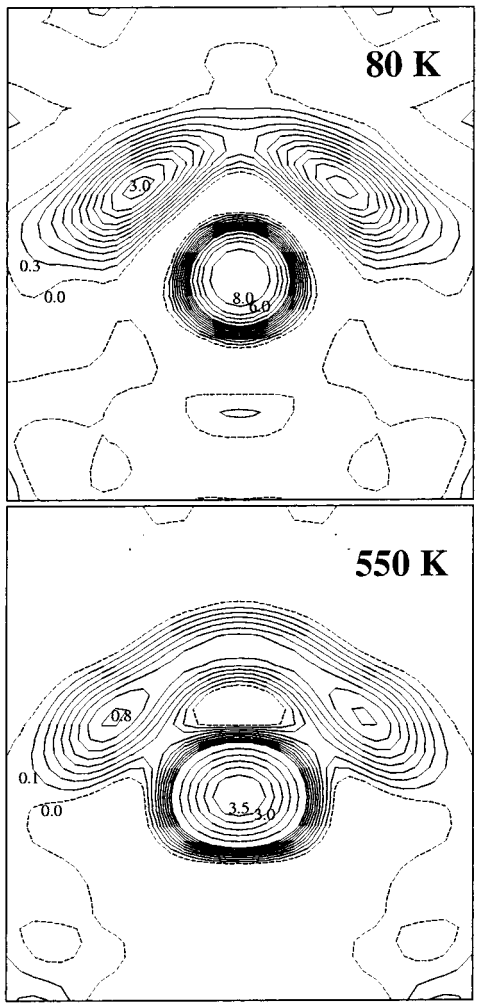

Figure 8. Fourier cuts of $Sr(ND_2)_2$ in the (010) plane at low and high temperatures. The center of reference is positioned at 0 1/4 0.130. The map size is 3.5 Å × 3.5 Å (*x*-axis = horizontal; *z*-axis = vertical).

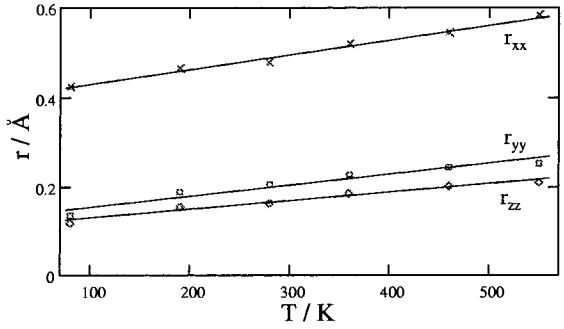

Figure 9. Temperature dependence of the rms displacements along the principal axis of the m.-s. displacement matrix of the deuterium atoms is pictured for $Sr(ND_2)_2$. r_{yy} represents the rms displacement perpendicular to the molecular plane of the amide ions and the principal axis corresponding to r_{zz} is aligned with the ND bond. The rms displacement described by r_{xx} is orientated perpendicular to the other two principal axes and faces the molecular plane of the amide ions.

TABLE 7: Relevant Refinement Parameters Obtained in Rietveld Profile Fits of the Neutron Diffraction Data of $Sr(ND_2)_2$ Using a Rigid-Body Model for the Amide Ions[a]

	80 K	190 K	293 K	360 K	460 K	550 K
refined site parameter of the center of mass on site 8e (0 $^1/_4$ z)						
z	0.1266(1)	0.1266(1)	0.1264(3)	0.1259(4)	0.1255(4)	0.1249(1)
refined elements of the translation matrix						
$\sqrt{T_{xx}}$/Å	0.214(4)	0.240(4)	0.213(8)	0.253(9)	0.272(11)	0.303(6)
$\sqrt{T_{yy}}$/Å	0.110(2)	0.133(3)	0.148(6)	0.176(6)	0.191(7)	0.188(4)
$\sqrt{T_{zz}}$/Å	0.137(4)	0.147(5)	0.141(7)	0.159(9)	0.160(10)	0.184(6)
refined elements of the libration matrix						
$\sqrt{L_{xx}}$/deg	2.0(3.0)	3.0(3.0)	4.1(4.0)	8.7(3.9)	15.4(4.0)	15.2(3.2)
$\sqrt{L_{yy}}$/deg	16.5(2.5)	18.0(2.5)	22.1(3.5)	24.9(3.6)	25.5(3.7)	25.8(3.0)
refined elements of the correlation matrix						
S_{xy}/Å deg	−1.31(5)	−1.59(6)	−0.89(17)	−1.04(19)	−1.43(19)	−1.43(7)
S_{yx}/Å deg	3.40(7)	4.00(7)	3.76(23)	3.89(28)	4.02(25)	4.98(9)
ND bond length corrected for amide ion librations using eq 1						
d_{ND}^{cor}/Å	1.035(3)	1.031(3)	1.034(8)	1.041(8)	1.046(8)	1.044(4)
anisotropic rms displacement of N calculated from **T**, **L**, and **S** using eq 2						
r_{xx}/Å	0.178	0.203	0.175	0.223	0.265	0.271
r_{yy}/Å	0.078	0.102	0.135	0.163	0.133	0.173
r_{zz}/Å	0.137	0.147	0.141	0.159	0.181	0.184
anisotropic rms displacement of D calculated from **T**, **L**, and **S** using eq 2						
r_{xx}/Å	0.418	0.455	0.473	0.515	0.560	0.575
r_{yy}/Å	0.183	0.209	0.198	0.227	0.239	0.266
r_{zz}/Å	0.117	0.131	0.135	0.179	0.192	0.205
(α β γ)	(0 323.9 0)	(0 324.3 0)	(0 318.7 0)	(0 318.2 0)	(0 322.4 0)	(0 321.6 0)

[a] The same notation as in Table 5 is used. Large librational amplitudes lead to a bent pdf and the average position is displaced inward when using an ellipsoid representation of the pdf. A correction of the ND bond lengths becomes necessary to achieve appropriate values. The correction value was calculated by means of the librational matrix expressed in its principal axis using the equation[48]

$$\delta\vec{r}_k = -\frac{1}{2}[(\mathrm{Tr}(\mathbf{L})\vec{r}_\kappa - \mathbf{L}r_\kappa)] \tag{1}$$

The anisotropic rms displacement parameters of N and D were calculated using equation[48]

$$\mathbf{U}_\kappa(\alpha) = \mathbf{T}(\alpha) + \mathbf{R}_\kappa(\alpha)\,\mathbf{L}(\alpha)(\mathbf{R}_\kappa(\alpha))^{\mathrm{T}} + \mathbf{S}(\alpha)(\mathbf{R}_\kappa(\alpha))^{\mathrm{T}} + \mathbf{R}_\kappa(\alpha)(\mathbf{S}(\alpha))^{\mathrm{T}} \tag{2}$$

$$\mathbf{R}_\kappa(\alpha) = \begin{pmatrix} 0 & r_3 & -r_2 \\ -r_3 & 0 & r_1 \\ r_2 & -r_1 & 0 \end{pmatrix}$$

of the amide ions (R_γ, wagging; R_t, twisting; R_r, rocking). The resulting pdf of a wagging libration is very similar to that of a twisting mode, especially for small m.-s. amplitudes. Due to finite resolution both librations are difficult to distinguish in diffraction experiments. To avoid correlations in our refinements, we took into account only the wagging libration and ignored the twisting mode. The corresponding value L_{zz} of the libration matrix was, therefore, set to zero and not refined. Thus, we have to work with seven parameters describing the thermal displacement of the "rigid" amide ions. This is also true for the standard model, but now we are much closer to lattice dynamics theory. The DND bond angle of the amide ions was fixed to 104° corresponding to its average value determined from the results of the unrestricted refinements (see Tables 5 and 6).

The R Bragg values of the rigid-body refinements do not get significantly worse. From the **T**, **L**, and **S** matrices we calculated the anisotropic displacement parameters of the nitrogen and deuterium atoms using eq 1. They fit well to corresponding values received with the standard model and are, therefore, a good prove for the relevance of the rigid-body model. Furthermore, the number of refinement parameters is 10 for the standard refinement and only 8 for the rigid-body refinement. The most important refinement parameters for both compounds are listed in Tables 7 and 8.

The elements of the translational tensor increase nearly linearly with rising temperature and correspond to the temperature dependence usually found in most crystalline compounds. More interesting is, however, the temperature dependence of the rms amplitudes of the normal librations L_{xx} (R_γ) and L_{yy} (R_r). Even at low temperatures the rms amplitude of the rocking libration is large and it increases only slightly with rising temperature. In contrast, the rms amplitude of the wagging libration at low temperatures is small and shows a strong increase with rising temperature (see Figure 10). The wagging libration starts to increase in the temperature region 300−360 K for $Sr(ND_2)_2$ and 300−380 K for $Ca(ND_2)_2$. In these regions the discrete change of the thermal expansion coefficient of the cell volume occurs as well. On the basis of these results, we assume a correlation between these two effects.

Another interesting point which follows from the rigid-body refinement is the participation of mixed vibrational modes in the dynamical processes of the amide ions. This can be concluded from elements S_{xy} and S_{yx} of the correlation matrix that are significantly different from zero. Attempts to neglect these parameters reduce the quality of the fit considerably. As mentioned above, the correlation matrix considers coupled translational and rotational degrees of freedom of the rigid molecular group. Due to the site symmetry of the center of mass of the amide ions correlations between translational and librational vibrations are restricted to the {100} planes. For more detailed investigations concerning this type of motion, further inelastic neutron-scattering experiments including a large energy range are necessary.

TABLE 8: Relevant Refinement Parameters Obtained in Rietveld Profile Fits of the Neutron Diffraction Data of $Ca(ND_2)_2$ Using a Rigid-Body Model for the Amide Ions. The Same Notation as in Table 7 Is Used

	100 K	200 K	293 K	380 K	460 K	555 K
refined site parameter of the center of mass on site 8e (0 $^1/_4$ z)						
z	0.1248(2)	0.1248(2)	0.1247(2)	0.1253(2)	0.1250(3)	0.1254(3)
refined elements of the translation matrix						
$\sqrt{T_{xx}}$/Å	0.189(8)	0.170(5)	0.188(5)	0.209(6)	0.211(7)	0.234(7)
$\sqrt{T_{yy}}$/Å	0.104(5)	0.135(4)	0.136(5)	0.173(5)	0.182(5)	0.201(5)
$\sqrt{T_{zz}}$/Å	0.142(5)	0.153(5)	0.165(4)	0.163(6)	0.154(6)	0.181(7)
refined elements of the libration matrix						
$\sqrt{L_{xx}}$/deg	3.6(3.5)	5.6(3.9)	4.5(4.0)	9.5(3.4)	13.3(3.5)	16.1(3.5)
$\sqrt{L_{yy}}$/deg	17.4(4.0)	18.8(4.0)	20.1(4.0)	23.9(4.0)	25.1(4.0)	28.2(4.0)
refined elements of the correlation matrix						
S_{xy}/Å deg	−1.73(11)	−1.46(11)	−1.69(11)	−1.74(19)	−1.99(22)	−1.45(24)
S_{yx}/Å deg	3.73(12)	2.88(12)	3.32(12)	3.23(22)	3.31(25)	3.18(26)
ND bond length corrected for amide ion librations using eq 1						
d_{ND}^{cor}/Å	1.027(8)	1.034(8)	1.031(8)	1.034(9)	1.035(9)	1.054(9)
anisotropic rms displacement of N calculated from **T**, **L**, and **S** using eq 2						
r_{xx}/Å	0.141	0.133	0.152	0.179	0.181	0.211
r_{yy}/Å	0.051	0.109	0.109	0.150	0.158	0.187
r_{zz}/Å	0.136	0.148	0.156	0.163	0.154	0.181
anisotropic rms displacement of D calculated from **T**, **L**, and **S** using eq 2						
r_{xx}/Å	0.429	0.415	0.445	0.482	0.494	0.534
r_{yy}/Å	0.201	0.209	0.215	0.252	0.276	0.283
r_{zz}/Å	0.099	0.127	0.142	0.152	0.160	0.194
(α β γ)	(0 322.4 0)	(0 316.6 0)	(0 316.4 0)	(0 316.2 0)	(0 316.0 0)	(0 316.1 0)

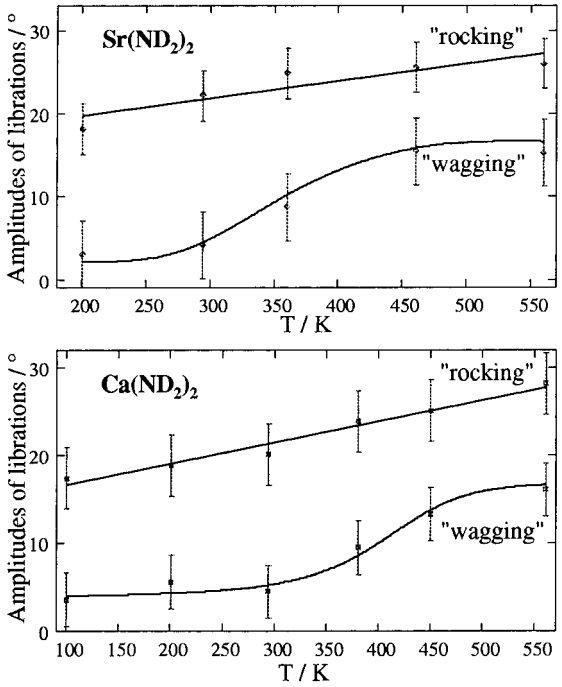

Figure 10. Rms amplitudes of the principal values L_{xx} and L_{yy} of the libration matrix in $Sr(ND_2)_2$ and $Ca(ND_2)_2$. They correspond to the amplitudes of the normal librations of the amide ions: $L_{xx} \simeq R_g$ (wagging) and $L_{yy} \simeq R_r$ (rocking). The solid lines show the trends of the data.

Additionally, we used the librational matrix to perform an appropriate bond length correction for the ND bond. The uncorrected bond lengths (see Tables 5 and 6) decrease with increasing temperature. The corrected values do not show any significant temperature dependence (see Tables 7 and 8) any longer. We calculated the average ND bond length to 1.037(9) Å. It is in the same range as a theoretical value based on ab initio Hartree−Fock calculation which yields 1.02 Å.[50]

Conclusions

For our experiments we first had to prepare about 10 g of radiographically and spectroscopically pure, fully deuterated compounds. This was reached by converting pure strontium and calcium metal in liquid ammonia under high pressure, respectively. Spectroscopic investigations showed that a percentage of hydrogen atoms in the deuterated compounds below 2% was achieved for all samples.

By means of high-resolution X-ray and neutron powder diffraction, the equilibrium positions for all atoms and the pdf of the amide ions were determined in a large temperature range. The results of these experiments as well as Raman and infrared spectroscopic measurements for both compounds are in good agreement with the structure model which was developed by Nagib, Kistrup, and Jacobs[27] for $Sr(ND_2)_2$.

However, a detailed study of the pdf shows that the orientational potential of the amide ions in $Sr(ND_2)_2$ and $Ca(ND_2)_2$ is strongly anisotropic. To underline this point, we calculated the Madelung part of the lattice energy (MAPLE) for different orientations of a central amide ion under the assumption that all other atoms are kept fixed on their equilibrium positions. Therefore, we designed a program[26] based on an algorithm described in ref 51. In Figure 11 the results of these calculations are given for small-angle rotations of the amide ion about the principal axes of the moment of inertia. As well as the distribution of the pdf, they show that the orientational potential of the "rocking" libration is much smaller and its mean amplitude is much larger than the corresponding values for the other two normal librations. Thus, the structure model could be considerably improved by introducing anisotropic m.-s. displacement parameters for the nitrogen and deuterium atoms in our refinements.

Quantitative values for the rms amplitude of the in-plane rotations of the amide ions represented by the "rocking" libration and the average amplitude of the out-of-plane rotations of the amide ions in this paper only described by the "wagging" librations were received by analyzing the anisotropic m.-s. displacement parameters of the nitrogen and deuterium atoms belonging to the same group by using a rigid-body model for the amide ion. So the librational modes were separated from the other types of motion. Even at low temperatures the mean amplitude of the rocking libration is large and it increases only slightly with rising temperature. In contrast, the mean amplitude of the wagging libration at low temperatures is small and shows

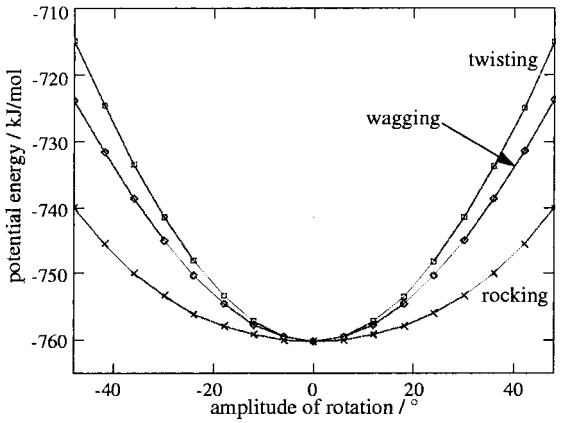

Figure 11. Influence of small-angle rotations of the amide ions about the principal axes of the moment of inertia. The calculation of the potential energy based on the MAPLE concept was carried out using the partial charges of +2.0 for the metal cations and +0.3 for the deuterium atoms. The partial charge used for the deuterium atoms was estimated from the dipole moment of the amide ion calculated by self-consistent field efforts.[50] This plot was extracted from the diffraction data of $Sr(ND_2)_2$ at 80 K.

a strong increase with rising temperature (see Figure 10). In the same temperature range a discrete change of the thermal expansion coefficients of the cell volume and the lattice parameters were observed (see Figures 3 and 4) by means of X-ray powder investigations. We assume a correlation between both effects. Furthermore, the rigid-body parametrization gives hints toward a rotation−translation coupling[52,53] for the dynamical processes of the amide ions. The elements of the libration matrix were used to correct the ND bond length of the amide ions which yields a temperature-independent value for both compounds. The average bond length was calculated to be 1.037(9) Å.

For a more detailed knowledge about dynamical processes in amide compounds, it would be interesting to study the above-mentioned phenomena with methods that are sensitive on the time scale of motion as well. Therefore, we also have carried out temperature-dependent solid-state NMR spectroscopic measurements and INS experiments using a small energy range to check for quasielastic scattering. This enabled us to study reorientational processes of the amide ions on a very large time scale. A complete treatise of these results including a comparison with the diffraction data will be presented in a forthcoming paper.

Acknowledgment. Financial support of this investigations by the German Bundesministerium für Bildung, Wissenschaft, Forschung und Technologie under Contract 03-JA4DOR-3 is acknowledged. Beam time as well as technical and scientific support were provided by the ISIS facility and the Hahn-Meitner-Institut, which is also gratefully acknowledged. The stay at the ISIS facility was supported within the HCM program of the European Commission.

References and Notes

(1) Bleif, H. J.; Dachs, H. *Acta Crystallogr.* **1982**, *A38*, 470.
(2) White, M. A.; Moore, S. A. *J. Chem. Phys.* **1986**, 85, 4629.
(3) Mach, B.; Jacobs, H.; Schaefer, W. *Z. Anorg. Allg. Chem.* **1987**, *553*, 187.
(4) Bastow, T. J.; Elcombe, M. M. *Solid State Commun.* **1986**, *59*, 257.
(5) Mach, B.; Jacobs, H.; Henning, J.; Lutz, H.-D. *Z. Anorg. Allg. Chem.* **1987**, *544*, 28.
(6) Mach, B.; Jacobs, H.; Harbrecht, B.; Henning, J.; Lutz, H.-D. *Z. Anorg. Allg. Chem.* **1987**, *544*, 55.
(7) Schotte, U.; Schotte, K. D.; Kabs, M.; Dachs, H. *J. Phys.: Condens. Matter* **1992**, *4*, 9283.
(8) Schotte, U.; Schotte, K. D.; Bleif, H.-J.; Kabs, M.; Dachs, H. *J. Phys.: Condens. Matter* **1995**, *7*, 7453.
(9) Ibers, J. A.; Kumato, J.; Snyder, R. G. *J. Chem. Phys.* **1960**, *33*, 1164.
(10) Ibers, J. A.; Kumato, J.; Snyder, R. G. *J. Chem. Phys.* **1960**, *33*, 1171.
(11) Lutz, H.-D. *Struct. Bonding* **1995**, *82*, 85.
(12) Juza, R.; Laurer, P. *Z. Anorg. Allg. Chem.* **1954**, *275*, 79.
(13) Kirchgässner, R. Dissertation Universität Dortmund, 1988.
(14) Jacobs, H.; Kirchgässner, R.; Bock, J. *Z. Anorg. Allg. Chem.* **1989**, *569*, 111.
(15) Metzner, U. Dissertation Universität Dortmund, 1989.
(16) Rush, J.; Livingstone, R. C.; Rosaco, G. *J. Solid State Commun.* **1973**, *13*, 159.
(17) Beckenkamp, K. Dissertation Gesamt-Hochschule Siegen, 1991.
(18) Rowe, J. M.; Livingstone, R. C.; Rush, J. J. *J. Chem. Phys.* **1973**, *58*, 5469.
(19) Seymour, R. S.; Pryor, A. W. *Acta Crystallogr.* **1970**, *B26*, 1487.
(20) Press, W. *Acta Crystallogr.* **1973**, *A29*, 257.
(21) Burandt, B.; Press, W.; Hausühl, S. *Phys. Rev. Lett.* **1993**, *71*, 1188.
(22) Hüller, A.; Kane, J. W. *J. Chem. Phys.* **1974**, *61*, 3599.
(23) Töpler, J.; Richter, D.; Springer, T. *J. Chem. Phys.* **1978**, *69*, 3170.
(24) Müller, M.; Senker, J.; Asmussen, B.; Press: W.; Jacobs, H.; Kockelmann, W.; Mayer, H. M.; Ibberson, R. M. *J. Chem. Phys.* **1997**, *107*, 2363.
(25) Müller, M. Dissertation Universität Kiel, 1996.
(26) Senker, J. Dissertation Universität Dortmund, 1996.
(27) Nagib, M.; Kistrup, H.; Jacobs, H. *Atomkernenergie* **1979**, *33*, 38.
(28) Juza, R.; Schumacher, H. *Z. Anorg. Allg. Chem.* **1963**, *324*, 278.
(29) Juza, R. *Angew. Chem.* **1964**, *7*, 290.
(30) Kistrup, H. Dissertation RWTH Aachen, 1975.
(31) Jacobs, H.; Schmidt, D. *Curr. Top. Mater. Sci.* **1982**, *8*, 379.
(32) Bock, J. Dissertation Universität Dortmund, 1986.
(33) Hüttig, G. F. *Z. Anorg. Allg. Chem.* **1920**, *114*, 161.
(34) Jeitschko, W.; Parthé, E.; Yvon, K. *J. Appl. Crystallogr.* **1977**, *10*, 73.
(35) Weidlein, Müller, Dehnicke; Schwingungsspektroskopie−Eine Einführung; Thieme Verlag: Stuttgart, 1988.
(36) Linde, G. Dissertation Universität Kiel, 1971.
(37) Bouclier, P.; Novak, A.; Portier, J.; Hagenmuller, P. *C. R. Acad. Sci. Paris* **1966**, *263C*, 875.
(38) Rousseau, D. L.; Bauman, R. P.; Porto, S. P. S. *J. Raman Spectrosc.* **1981**, *10*, 253.
(39) Neutron-Scattering Instrumentation at the upgraded Research Reactor BER II.; Hahn-Meitner-Institut Berlin, 1996.
(40) Experimental Report ISIS Rutherford Appleton Laboratory, 1996.
(41) Larson, A. C.; Dreele, R. B. Program GSAS General Structure Analysis System; Los Alamos National Laboratory, Los Alamos, NM, 1994.
(42) Young, R. A. *The Rietveld Method*; International Union of Crystallography; Oxford University Press: London, 1993.
(43) Rietveld, H. M. *Acta Crystallogr.* **1967**, *22*, 151.
(44) Rietveld, H. M. *Appl. Crystallogr.* **1969**, *2*, 65.
(45) Howard, C. J. J. *Appl. Crystallogr.* **1982**, *15*, 615.
(46) Brink, D. M.; Sachtler, G. R. *Angular momentum*; Oxford University Press: London, 1962.
(47) Shomaker, V.; Trueblood, K. *Acta Crystallogr.* **1968**, *B24*, 63.
(48) Willis, B. T. M.; Pryor, A. W. *Thermal Vibrations in Crystallography*; Cambridge University Press: Cambridge, 1975.
(49) Cyvin, S. J. *Molecular Vibrations and Mean Square Amplitudes*; Elsevier Publishing Company: Amsterdam, 1968.
(50) Lee, T. J.; Schaefer, H. F. *J. Chem. Phys.* **1985**, *83*, 1784.
(51) Hellwege, K. H. *Einführung in die Festkörperphysik*; Springer-Verlag: Berlin, Heidelberg, 1991
(52) Schiebel, P.; Hoser, A.; Prandl, W.; Heger, G. *Z. Phys. B−Condensed Matter* **1990**, *81*, 253.
(53) Schiebel, P.; Hoser, A.; Prandl, W.; Heger, G.; Paulus, W.; Schweiss, P. *Z. Phys. B−Condensed Matter* **1994**, *6*, 10989.
(54) The probability density function (pdf) $p_\varkappa(\vec{u})$ is defined as the probability of finding an atom $\varkappa$ in the volume element d^3u when it is displaced by $\vec{u}$ from its rest position.